Available online at www.sciencedirect.com

ScienceDirect

Procedia Engineering 120 (2015) 824 – 827

Procedia Engineering

www.elsevier.com/locate/procedia

EUROSENSORS 2015

Functional multisensor for temperature and subsequent 3D magnetic-field measurement

S. V. Lozanova, S. A. Noykov, A. J. Ivanov, Ch. S. Roumenin*

Institute of Systems Engineering and Robotics at Bulgarian Academy of Sciences, Block 2, Acad. G.Bonchev St. 1113 Sofia, BULGARIA

Abstract

A novel functional multisensor for temperature and subsequent measurement of three orthogonal magnetic-field components using the same transducer zone is presented. One central emitter, two symmetrically positioned base contacts and two pairs of output ohmic terminals on a silicon substrate, close to the bases, are implemented. Three subsequent coupling arrangements of the output terminals use the same element at different times. Temperature is measured through the voltage on the forward biased p^+-n emitter junction at constant supply current. The channel sensitivities are $S_x = 7$ V/AT, $S_y = 9$ V/AT and $S_z = 11.3$ V/AT. The thermo-sensitivity is $K_{EB} = 1.82$ mV/ºC at supply current of 1 mA. Magnetic induction does not perturb thermometric voltage within a wide range, - 0.8 T $\leq B \leq$ 0.8 T. The spatial resolution reaches about 110 x 90 x 40 μm^3.

Peer-review under responsibility of the organizing committee of EUROSENSORS 2015

Keywords: 3-D Hall sensing; subsequent measurement method; magnetic-field instrumentation

1. Introduction

The metrological data about all of the three orthogonal components B_x, B_y and B_z of the magnetic field vector B always refer to some coordinate system. This is the only correct approach to the study of processes and phenomena, for which this nature-universal parameter is responsible. The most widespread method in vector magnetometry, along with accompanying devices and technological solutions, constitutes an element integration of three orthogonal magnetic-field transducers, such as Hall microsensors, magnetotransistors and magnetodiodes onto a common silicon substrate [1-4]. In spite of the perfect differentiation of the simultaneously obtained data for the components

* Corresponding author. Tel.: +359 2 870 33 61
E-mail address: roumenin@bas.bg

Peer-review under responsibility of the organizing committee of EUROSENSORS 2015
doi:10.1016/j.proeng.2015.08.683

B_x, B_y and B_z, the most advanced 3D silicon magnetometers feature some drawbacks. They contain many contacts and numerous electrical connections between them. Another important problem arises from the need to compensate the strong temperature dependence of the characteristics of the multidimensional MEMS, which requires a thermometric signal from an additional sensor. For these reasons, it is difficult to fulfill the main requirement for high spatial resolution capability (measurement in a "spot"). These disadvantages complicate technology fabrication and impede the overall accuracy. One promising means overcoming these significant problems is the multisensor principle – obtaining of sensor data, which characterize different existing phenomena in the same transducer region [1]. For example, in low-frequency magnetometry, it is very easy to select high enough frequency f_0, such that $f_0 >> f$, where: f_0 is the rate of commutation between three subsequent sensor configurations – for detecting B_x, B_y and B_z, respectively; f is the maximal frequency of changing the magnitude and/or the direction of the magnetic field B [5]. This innovative idea is the basis of solutions, where the same substrate is used to measure the field B – in fact, the metrological task is expanded in time but not in space. A novel 3D functional multisensor measuring the temperature and subsequently, the magnetic-field components, where the mentioned drawbacks are successfully reduced, is presented.

2. Device design and working principles

The integrated 3D sensor basically contains one central p^+-n emitter junction E, two adjacent symmetrically positioned n^+-n base contacts B_1-B_2 and two pairs of output n^+-n Hall terminals, H_1-H_2 and H_3-H_4, close to the bases B_1 and B_2, Fig. 1. All of them are surrounded by a deep rectangular p-ring. This ring restricts surface current spread and confines the transducer region in the bulk. The experimental prototype has been implemented using bipolar IC process. The sizes of emitter E and base contacts B_1 and B_2 are 20 x 20 μm^2 and 60 x 10 μm^2, respectively. The dimensions of the four output ohmic terminals H_1…H_4 are 10 x 5 μm^2, the depth of all heavily doped n^+ and p^+ regions is about 1 μm and the doping concentration is 10^{20} cm^{-3}. The p-ring width at the surface is about 25 μm. The substrate dopant donor concentration is $N_D = n_0 = 4.3 \times 10^{15}$ cm^{-3}, i.e. the chip resistivity is $\rho \approx 7.5$ Ω.cm. The holes injected into the bulk by the forward-biased emitter junction E spread out towards the base contacts B_1 and B_2. Simultaneously, to neutralize the positive charges of the holes, the same number of majority electrons enters into the base region of the two long-base width W_b diodes E-B_1 and E-B_2, $W_b > L_p$, where L_p is the diffusion length. The hole-generated current flows in the vicinity of the emitter E. The current due to drift electrons flows in the vicinity of the two base contacts B_1 и B_2 and the output terminals H_1…H_4. In the zone of the contacts B_1 and B_2, the accelerating field of the energy supply acts.

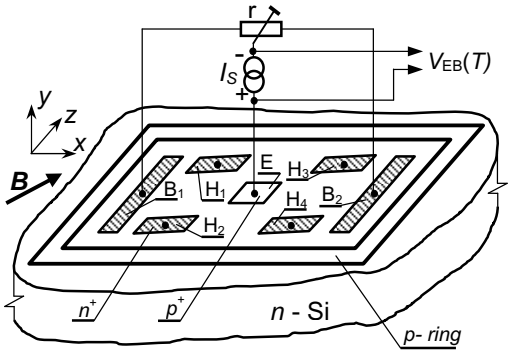

Fig. 1. 3-D multisensor measuring the full magnetic-field vector and temperature. The trimmer r serves as offset channels compensation.

The device operation is determined by the nonlinearity of the carriers' trajectory [1, 5]. Initially, the electrons under bases B_1 and B_2 flow vertically in the bulk, then their direction becomes parallel to the surface, afterwards the hole current predominates around the emitter E. The sensor action is based on the majority carrier deflection, caused by the Lorentz force $\boldsymbol{F}_L$ ($\boldsymbol{F}_{Lx}$, $\boldsymbol{F}_{Ly}$, $\boldsymbol{F}_{Lz}$) in accordance with the orthogonal fields $\boldsymbol{B}_x$, $\boldsymbol{B}_y$ and $\boldsymbol{B}_z$. The output differential voltages for each of the magnetic field components are obtained by means of the innovative construction and the three subsequent combinations of connections of the terminals H_1...H_4, Fig. 2. In field $\boldsymbol{B}_x$, the Lorentz force

$\boldsymbol{F}_{L,z} = q\boldsymbol{v}_{dr,y} \times \boldsymbol{B}_x$ acts on the majority carrier velocity $\boldsymbol{v}_{dr,y}$, generating Hall potentials on the upper surface in the vicinity of terminals H_1-H_2 and H_3-H_4, where q is the elementary charge. Thus, voltages $V_{H1,2}$ and $V_{H3,4}$ are equal in value. The arrangement in Fig. 2a accomplishes parallel connection of these signals. The magnetosensitivity along the y axis, Fig. 1, is determined by Lorentz deflection of the carriers in the plane x-z: $\boldsymbol{F}_{L,z} = q\boldsymbol{v}_{dr,x} \times \boldsymbol{B}_y$. Thus, on Hall terminals H_1-H_2 and H_3-H_4 in the field $\boldsymbol{B}_y$, additional potentials of the same value and opposite sign are generated. The information about the component $\boldsymbol{B}_y$ is obtained by the Hall voltage $V_{H,y}$ and the arrangement from Fig. 2b. The magnetosensitivity along the z axis is determined by the carrier deflection in the plane x-y: $\boldsymbol{F}_{L,x} = q\boldsymbol{v}_{dr,x} \times \boldsymbol{B}_z$ and $\boldsymbol{F}_{L,y} = q\boldsymbol{v}_{dr,x} \times \boldsymbol{B}_z$, i.e. the transducer efficiency is determined by the velocities $v_{dr,x}$ and $v_{dr,y}$. Due to the Lorenz forces, the symmetrical current trajectories are deformed. The information about the component $\boldsymbol{B}_z$ is obtained by the Hall voltage $V_{H,z}$ and the arrangement from Fig. 2c. The thermometric dependence of the diode bias $V_{EB}(T)$ at constant current I_{EB} = const is linear [1]. The sensitivity coefficient $K_{p\text{-}n} \equiv K_{EB} = \partial V_{EB}/\partial T$ is negative and, depending on the value of the emitter current I_E, reaches in first approximation no more than $K_{EB} \approx$ - 2 mV/ºC. By means of subsequent switching between the three arrangements, presented in Fig. 2, complete information about all three components of magnetic vector $\boldsymbol{B}$ is obtained, as the voltage $V_{EB}(T)$ is the required signal for thermocompensation of all three magnetosensitivities S_x, S_y and S_z, and offsets drift. The multiplexer repetition frequency of these arrangements from Fig. 2 must be sufficiently high, so as not to change field $\boldsymbol{B}$.

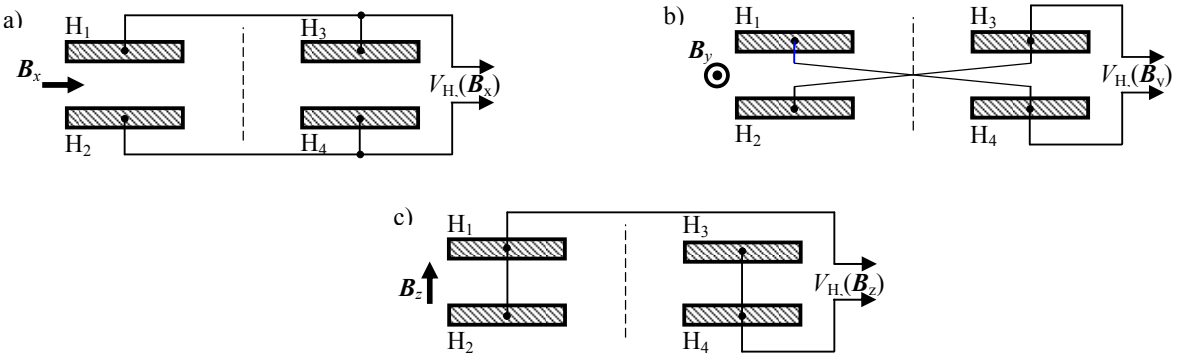

Fig. 2. Three connection arrangements of contacts $H_1 \ldots H_4$ for subsequent measurement of components $\boldsymbol{B}_x$, $\boldsymbol{B}_y$ and $\boldsymbol{B}_z$.

3. Experimental results

The output 3D magnetometer characteristics are shown in Fig. 3(a). The obtained relative channel sensitivities are S_x = 7 V/AT, S_y = 9 V/AT and S_z = 11.3 V/AT, respectively. The lower transducing efficiency in comparison with other 3D sensors results from bipolar conductivity. The new multisensor provides small channel cross-sensitivity appropriate for precise measurement, Fig. 3(b). Figure 4(a) presents the experimental results of the linear temperature dependence of the emitter-base bias $V_{EB}(T)$. With increase of current I_{EB}, thermo-sensitivity K_{EB} decreases. Experimentally is proved that magnetic induction B does not perturb thermometric voltage $V_{EB}(T)$ in the range - 0.8 T $\leq B \leq$ 0.8 T. The signal $V_{EB}(T)$ is required for full temperature compensation of the sensitivities and offsets drift at the next stage of conditioning circuitry to improve the accuracy. In Fig. 4(b), the behaviour of internal channel V_{Hz} noise is presented. The spectral density of the noise for the other two channels is practically the same. The spectrum in the range 10 Hz $\leq f \leq$ 1 kHz is of 1/f type. The resolution is high, reaching 110 x 90 x 40 μm^3.

4. Conclusion

The achieved performance of the 3D multisensor is the progress of the subsequent method for measurement of magnetic-field components using the same transducer zone. The possibilities are extended by obtaining of information about the chip temperature, required to compensate the sensitivity of offsets drift. The applications of the novel magnetometer comprise robotics, microdevices for measuring angular and linear displacements, etc.

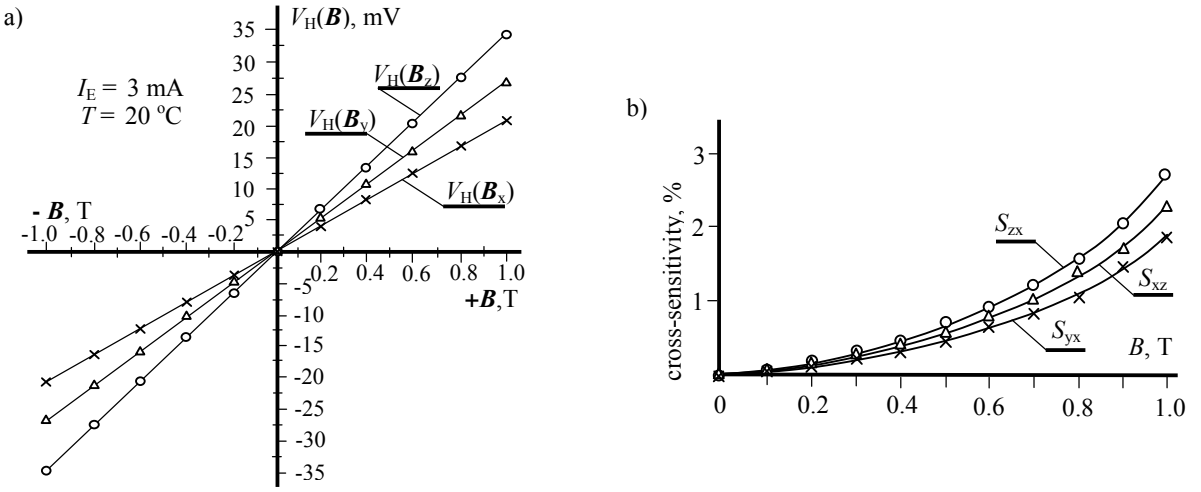

Fig. 3. (a) Output Hall voltages at fully compensated offsets; (b) Channel crosstalk as a function of induction $\boldsymbol{B}$ at temperature T = 20 ºC.

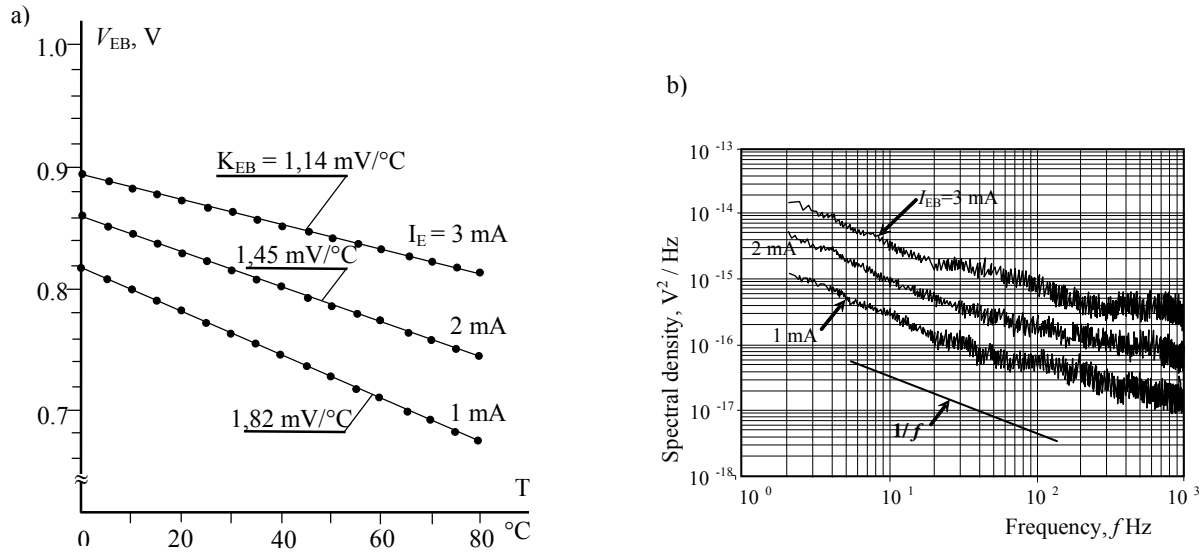

Fig. 4. (a) Temperature dependence of the bias V_{EB}, induction B = 0.6 T; (b) Spectral density of internal noise for $\boldsymbol{B}_z$-channel, T = 20 ºC.

References

[1] C. Roumenin, Microsensors for magnetic field, in J.G. Korvink and O. Paul, eds, MEMS – a practical guide to design, analysis and application, W. Andrew Publ., USA & Spriger, pp. 453-521, 2006.
[2] E. Ramsden, Hall effect sensors – Theory and application, 2nd ed., Elsevier, Netherland, 2006.
[3] F. Burger, P-A. Besse, R. Popovic, New fully integrated 3-D silicon Hall sensor for precise angular-position measurement, Sens. Actuators A, 67 (1998) 72-76.
[4] C. Sander, C. Leube, T. Aftab, P. Ruther, O. Paul, Isotropic 3D silicon Hall sensor, Proc. of MEMS 2015, Estoril, Portugal, 893-896, 2015.
[5] S. Lozanova, S. Noykov, C. Roumenin, A novel 3-D Hall magnetometer using subsequent measurement method, Sens. Actuators, A, 153 (2009) 205-211.